HHS Public Access

Author manuscript

J Bone Miner Metab. Author manuscript; available in PMC 2014 September 01.

Published in final edited form as:

J Bone Miner Metab. 2013 September ; 31(5): 520–532. doi:10.1007/s00774-013-0449-6.

RhoA GTPase interacts with beta-catenin signaling in clinorotated osteoblasts

Qiaoqiao Wan, **Eunhye Cho**, **Hiroki Yokota**, and **Sungsoo Na***

Department of Biomedical Engineering, Indiana University-Purdue University Indianapolis, Indianapolis, IN 46202 USA

Abstract

Bone is a dynamic tissue under constant remodeling in response to various signals including mechanical loading. A lack of proper mechanical loading induces disuse osteoporosis that reduces bone mass and structural integrity. β-catenin signaling together with a network of GTPases is known to play a primary role in load-driven bone formation, but little is known about potential interactions of β-catenin signaling and GTPases in bone loss. In this study, we addressed a question: Does unloading suppress an activation level of RhoA GTPase and β-catenin signaling in osteoblasts? If yes, what is the role of RhoA GTPase and actin filaments in osteoblasts in regulating β-catenin signaling? Using a fluorescence resonance energy transfer (FRET) technique with a biosensor for RhoA together with a fluorescent T-cell factor/lymphoid enhancer factor (TCF/LEF) reporter, we examined the effects of clinostat-driven simulated unloading. The results revealed that both RhoA activity and TCF/LEF activity were downregulated by unloading. Reduction in RhoA activity was correlated to a decrease in cytoskeletal organization of actin filaments. Inhibition of β-catenin signaling blocked unloading-induced RhoA suppression, and dominant negative RhoA inhibited TCF/LEF suppression. On the other hand, a constitutively active RhoA enhanced unloading-induced reduction of TCF/LEF activity. The TCF/LEF suppression by unloading was enhanced by co-culture with osteocytes, but it was independent on organization of actin filaments, myosin II activity, or a myosin light chain kinase. Collectively, the results suggest that β-catenin signaling is required for unloading-driven regulation of RhoA, and RhoA, but not actin cytoskeleton or intracellular tension, mediates the responsiveness of β-catenin signaling to unloading.

Keywords

fluorescence resonance energy transfer (FRET); RhoA; T-cell factor/lymphoid enhancer factor (TCF/LEF); unloading; mechanotransduction

***Corresponding author**. Sungsoo Na, PhD, Department of Biomedical Engineering, Indiana University-Purdue University Indianapolis, 723 West Michigan Street, SL220G, Indianapolis, IN 46202, USA, Phone: 1-317-278-2384, Fax: 1-317-278-2455, sungna@iupui.edu.

Conflict of Interest

All authors have no conflicts of interest.

Introduction

Mechanical loading plays a critical role in bone remodeling, and unloading due to bed rest and weightlessness in space reduces bone mass and structural strength [1–4]. For a mechanism of load-driven enhancement of bone formation, many lines of evidence support the role of β-catenin signaling. The β-catenin-dependent Wnt signaling plays an important role in bone formation [5] and fracture healing [6]. It is reported that mechanical loading induces a translocation of active β-catenin to the nucleus [7,8], followed by interaction with T-cell factor/lymphoid enhancer factor (TCF/LEF) transcription factors, leading to the activation of Wnt-responsive genes [9–11]. In addition, *in vivo* studies using mice show that mechanical loading increases the level of Wnt/β-catenin signaling activity [12,13].

RhoA is a member of the Rho family of GTPases, which encode fundamental cellular processes such as cell differentiation, migration, as well as the assembly and organization of the actin cytoskeleton [14,15]. RhoA is involved in osteoblastic cell survival [16], bone resorption [17] and inhibition of bone morphogenetic protein-2 [18]. In response to shear stress, RhoA is activated in osteoblasts [19] and its activation stimulates the formation of actin cytoskeleton that enhances mechanosensitivity [20,21]. Despite load-driven activation of β-catenin signaling and RhoA GTPase in osteoblasts, little is known about their responses to unloading. A primary aim of this study was to examine the role of β-catenin signaling and RhoA activities and their interaction in osteoblasts under simulated unloading.

Clinorotation has been widely used as a simulated model of unloading or microgravity for *in vitro* studies [22–26]. The method does not generate any weightlessness condition but it moves a fixed direction of gravitational forces by rotating a culture chamber, which results in a vector-averaged reduction in the apparent gravity on the cell culture. In this study, we addressed questions using clinorotated osteoblasts: Does clinorotation reduce β-catenin signaling and RhoA GTPase activity in osteoblasts? If yes, what is the role of RhoA GTPase and actin cytoskeletal organization in regulating β-catenin signaling in osteoblasts under clinorotation? To answer to these questions, we employed a fluorescence energy transfer (FRET) technique using a RhoA GTPase biosensor together with a fluorescent TCF/LEF reporter and examined the effects of clinorotation on RhoA activity and β-catenin-linked transcription activity in osteoblasts and the molecular signaling pathways that link the two. Osteoblasts were transfected with these probes and thus both RhoA activity and β-catenin driven TCF/LEF activity were determined in individual cells. To explore the role of RhoA and actin cytoskeletal organization, we used RhoA mutants and pharmacological drugs that inhibit actin cytoskeletal organization, actin-myosin interaction, or myosin light chain kinase. As a positive control of mechanical stimulation, we employed fluid flow-driven shear stress and examined TCF/LEF transcriptional responses in osteoblasts. To evaluate the role of osteocytes in mechanotransduction of osteoblasts, experiments were conducted with and without co-culturing osteocytes in the chamber.

Materials and methods

DNA plasmids

We used a FRET-based, cyan fluorescent protein (CFP)-yellow fluorescent protein (YFP) RhoA biosensor [27]. The probe consists of truncated RhoA, a RhoA binding domain, and a pair of CFP and YFP. Changes in RhoA activity cause a conformational change of the biosensor, leading to a change in FRET efficiency between CFP and YFP of the RhoA biosensor. Thus, RhoA activity can be visualized as changes in the emission intensity ratio of YFP/CFP. The RhoA biosensor has been well characterized in terms of its specificity [27–29]. As RhoA mutants, a constitutively active RhoA (RhoA-V14) and a dominant negative RhoA (RhoA-N19) were used [30]. To evaluate the effects of simulated unloading on β-catenin signaling, we used the TCF/LEF-green fluorescent protein (GFP) reporter (SA Biosciences, Valencia, CA, USA). This reporter utilizes the inducible transcription factor-responsive GFP that encodes the GFP gene under the control of a basal promoter element joined to tandem repeats of the TCF/LEF transcriptional response element. Thus, GFP intensity can be used as a measure of TCF/LEF activity. An mCherry-actin probe was used to monitor the changes in actin cytoskeleton under simulated unloading and shear stress application [31].

Cell culture and transfection

Mouse osteoblast-like MC3T3-E1 cells (ATCC, Manassas, VA, USA) were cultured in minimum essential alpha medium (αMEM; Invitrogen, Grand Island, NY, USA) containing 10% FBS (Hyclone, South Logan, UT, USA) and antibiotics (50 units/ml penicillin and 50 μg/ml streptomycin; Lonza, Basel, Switzerland). Preosteocyte-like MLO-A5 cells were cultured in αMEM containing 5% calf serum (Hyclone), 5% FBS and penicillin/streptomycin [32]. Prior to experiments, the cells were maintained at 37°C and 5% CO_2 in a humidified incubator. The DNA plasmids were transfected into the cells using a Neon transfection system (Invitrogen). After transfection, the cells were transferred to a type I collagen-coated μ-slide cell culture chamber (Ibidi, Verona, WI, USA) and incubated in αMEM containing 0.5% FBS for 24–36 h before imaging experiments.

Inhibitors

Cytochalasin D (1 μg/ml; Enzo Life Sciences, Farmingdale, NY, USA) was used to disrupt actin filaments. Blebbistatin (50 μM; Toronto Research Chemicals, Toronto, Ontario, Canada) was used to inhibit myosin II activity. ML-7 (25 μM; Enzo Life Sciences, Farmingdale, NY, USA) was used to inhibit myosin light chain kinase. XAV939 (1 mM; R&D Systems, Minneapolis, MN, USA) was used to inhibit Wnt/β-catenin signaling. A cell permeable Rho inhibitor (1 μg/ml; Cytoskeleton, Denver, CO, USA) was used to inhibit RhoA activity.

Clinorotation for simulated unloading

We used a custom-made incubator equipped with a rotating platform that holds a cell culture chamber (Fig. 1A). The unloading condition (0.005 g) was simulated by rotating the cell culture chamber (Ibidi, Verona, WI, USA) longitudinally at 15 rpm [33]. Two ports of the

cell culture chamber were connected with syringe filters (Whatman, Piscataway, NJ, USA) to allow gas exchange. For time-lapse imaging during clinorotation, the culture chamber was dismounted from the rotating platform in the incubator and placed on the microscope stage to measure RhoA activity, actin cytoskeletal remodeling, and TCF/LEF activity. After image acquisition, the cell culture chamber was removed from the microscope stage and mounted on the rotating platform. During clinorotation experiments, the cells were maintained in HEPES-buffered (20 mM) αMEM without serum at 37°C and images were taken for 4 h at an interval of 30 min.

Shear stress application

As a positive control experiment for mechanical stimulation of MC3T3-E1 cells, an oscillatory (1 Hz) shear stress at 10 dyn/cm^2 was applied to the cell culture chamber (Ibidi, Verona, WI, USA) by using a peristaltic pump (Cole-Parmer, Vernon Hills, IL, USA) and an Osci-Flow device (Flexcell International, Hillsborough, NC, USA). During shear stress application, images were taken for 1 h at an interval of 10 min. The flow experiments were conducted at 37°C and the cells were maintained with serum-deprived αMEM containing 20 mM HEPES.

Microscopy and image acquisition

Images were obtained by using an automated fluorescence microscope (Nikon Instruments, Melville, NY, USA) equipped with a charge-coupled device camera (Evolve 512; Photometrics, Tucson, AZ, USA), a filter wheel controller (Sutter Instruments, Novato, CA, USA) and a Perfect Focus System (Nikon) that maintained the focus during time-lapse imaging. The following filter sets were used (Semrock, Rochester, NY, USA): CFP excitation: 438/24 (center wavelength/bandwidth in nm); CFP emission: 483/32; YFP (FRET) emission: 542/27; mCherry excitation: 562/40; mCherry emission: 641/75; GFP excitation: 472/30; GFP emission: 520/35. Cells were illuminated with a 100 W Hg lamp through an ND64 (~1.5% transmittance) neutral density filter to minimize photobleaching. During clinorotation and shear stress experiments, time-lapse images were acquired at an interval of 30 min and 2 min, respectively. The images were taken from the same cell for each imaging experiment. A 40X objective lens (0.75 numerical aperture; Nikon) was used for all imaging experiments. FRET images for RhoA activity were generated with NIS-Elements software (Nikon) by computing emission ratio of YFP/CFP for the individual cell. The quantification of TCF/LEF activity was conducted using NIS-Elements software. The individual cell area was obtained from DIC images. The GFP images were background-subtracted and the GFP intensities were averaged over the whole cell area. We performed static control experiments using RhoA and TCF/LEF probes without applying clinorotation or shear stress and confirmed that there was no photo-bleaching during imaging experiments (Fig. 2).

Statistical analysis

At least five independent experiments were performed for each condition. YFP/CFP emission ratios and fluorescence intensity data were normalized by their basal levels before stimulation in the same cell. Statistical analyses were performed using Prism 5 software (GraphPad Software, La Jolla, CA, USA). Data were presented as the mean ± standard error

of the mean (SEM). One-way analysis of variance followed by Dunnett's test and Tukey's test were used to determine the statistical differences for time course experiments and multiple comparisons, respectively. Student's *t*-test was used to compare two groups. The *P*-value less than 0.05 was considered significant.

Results

Simulated unloading by clinorotation induces a sustained suppression of RhoA activity

The initial experiments were designed to determine whether RhoA would be regulated under clinorotation. For these experiments, MC3T3-E1 cells were transfected with a FRET-based CFP-YFP RhoA biosensor and spatiotemporal activities of RhoA in the cells were monitored during 4 h of clinorotation. RhoA activity was decreased within 2 h after onset of clinorotation as evidenced by the significant changes (~10%) in FRET ratio (YFP/CFP) and the decreased level of RhoA activity was maintained during the clinorotation experiment (Fig. 1B and 1C). We also confirmed using the Rho inhibitor that Rho inhibition prevented clinorotation-induced RhoA suppression (Fig. 1C). These data show the significant role of the unloading condition in RhoA GTPase activity in osteoblasts.

RhoA suppression by clinorotation is associated with decreased actin cytoskeleton

Since RhoA is known to regulate actin cytoskeletal organization [14], we examined whether simulated unloading-driven RhoA activity would affect actin cytoskeleton structure and distribution. We transfected MC3T3-E1 cells with mCherry-actin and monitored the actin cytoskeleton over the course of the experiment. In MC3T3-E1 cells, actin stress fibers gradually disappeared and actin GFP intensity was significantly decreased during clinorotation (Fig. 1D and 1E). These data show that a decrease in actin stress fibers by simulated unloading is closely associated with the RhoA activity.

Clinorotation downregulates β-catenin signaling activity

Bone formation in response to mechanical loading is closely associated with β-catenin signaling [13] and unloading leads to bone loss [3,34]. To visualize the activity of β-catenin signaling under simulated unloading, we used the TCF/LEF-GFP reporter since β-catenin activation is known to lead to TCF/LEF transcriptional activation [35]. The TCF/LEF-GFP reporter increases the GFP intensity level in the cytoplasm when activated β-catenin forms a complex with TCF/LEF transcription factors. We transfected MC3T3-E1 cells with the TCF/LEF reporter and measured the GFP intensity in the cytoplasm as an indicator of β-catenin signaling activity. The GFP intensity level was significantly decreased at 2.5 h (23%), followed by a further decrease at 3.5 h (40%) (Fig. 3A, B). These results indicate that simulated unloading by clinorotation reduces β-catenin signaling activity of MC3T3-E1 cells.

A decrease in β-catenin signaling activity by clinorotation is independent of the actin cytoskeleton and intracellular tension

Microgravity condition was shown to affect cell morphology and cytoskeletal structure [36–38]. To examine the role of actin cytoskeleton in β-catenin signaling, cytochalasin D (CytoD) was applied. CytoD treatment did not affect TCF/LEF activity by clinorotation.

Blebbistatin (Bleb) and ML-7 that inhibit myosin II activity and myosin light chain kinase (MLCK), respectively, also failed to affect TCF/LEF activity by clinorotation (Fig. 3C). We further examined whether these drugs could affect the basal level of TCF/LEF activity. The treatment of CytoD, Bleb, or ML-7 did not induce any changes in the basal TCF/LEF activity (Fig. 3D). These results suggest that a decrease in β-catenin signaling activity by simulated unloading in MC3T3-E1 cells is independent of actin cytoskeleton organization and MLCK/myosin activity.

β-catenin signaling is required for clinorotation-induced RhoA suppression

To examine the effects of β-catenin signaling to RhoA GTPase activity, we used XAV939, an inhibitor of Wnt/β-catenin signaling. The XAV939 acts as an inhibitor of tankyrase to stabilize axin, which in turn stimulates β-catenin degradation and inhibits β-catenin-mediated transcription [39]. First, we tested whether XAV939 could block TCF/LEF activity under clinorotation. We first transfected MC3T3-E1 cells with TCF/LEF biosensor and treated them with XAV939. XAV939 treatment totally blocked TCF/LEF activity (Fig. 4A). Next, we examined the role of β-catenin in clinostat-induced RhoA activity. We transfected the cells with RhoA biosensor and then treated with XAV939. XAV939 completely blocked RhoA suppression during clinorotation (Fig. 4B, C). Interestingly, inhibition of Wnt/β-catenin signaling using XAV939 reduced the basal activity of RhoA (Fig. 4D). Together, these data suggest that the basal level RhoA activation is in part due to endogenous Wnt/β-catenin signaling and that β-catenin signaling is required for simulated unloading-induced RhoA regulation.

Constitutively active RhoA enhances downregulation of β-catenin signaling activity during clinorotation by increasing the basal level of β-catenin signaling activity

While the role of β-catenin signaling in RhoA has been well documented [40], the role of RhoA in β-catenin signaling under unloading is not well understood. To assess the potential effects of RhoA on β-catenin signaling under clinorotation, we co-transfected MC3T3-E1 cells with a TCF/LEF reporter and a constitutively active RhoA (RhoA-V14) or a dominant negative RhoA (RhoA-N19). The basal TCF/LEF activity in the RhoA-V14-transfected cells was higher than that in the control cells, whereas the basal TCF/LEF activity in the RhoA-N19-transfected cells was lower than that in the control cells (Fig. 5A). The cells expressing constitutively active RhoA exhibited a substantial reduction (>50%) in TCF/LEF activity within 1.5 h of clinorotation (Fig. 5B, C). The reduction shown in the RhoA-V14-transfected cells was faster (1.5 h versus 3.5 h) and larger (>50% versus 40%) than that in the wildtype control cells (Fig. 5C versus Fig. 3B). However, the dominant negative RhoA completely abolished the reduction of TCF/LEF activity by clinorotation (Fig. 5D). The enhanced reduction of TCF/LEF activity in cells transfected with RhoA-V14 might be due to the higher basal level of TCF/LEF activity in the cells (Fig. 5A). These results suggest that RhoA mediates the responsiveness of β-catenin signaling to simulated unloading by modulating the basal level of TCF/LEF activity.

Flow-induced shear stress increases β-catenin signaling activity

As a positive control for simulated unloading, we performed shear stress experiments and monitored TCF/LEF activity and actin cytoskeletal remodeling. First, we transfected

MC3T3-E1 cells with a TCF/LEF reporter and visualized its activity while applying oscillatory (1 Hz) shear stress at 10 dyn/cm^2. Shear stress gradually increased TCF/LEF activity and its increase became significant at 40 min of shear stress (Fig. 6A and 5B). Next, we transfected MC3T3-E1 cells with mCherry-actin and monitored actin cytoskeletal remodeling under shear stress. In contrast to clinorotation data, actin stress fibers were increased during shear stress application (Fig. 6C). Consistent with previous reports [8,21,41], these results suggest a stimulatory role for shear stress in β-catenin signaling activity and actin cytoskeleton organization.

Osteocytes enhance unloading driven suppression of β-catenin signaling activity in osteoblasts

Increasing evidence suggests that β-catenin-dependent Wnt signaling in osteoblasts is regulated by sclerostin, which is exclusively made by osteocytes and inhibits the activation of Wnt/β-catenin signaling [42]. To test the effects of osteocytes on β-catenin signaling in osteoblasts, we transfected MC3T3-E1 cells with a TCF/LEF reporter and cultured them with non-transfected MLO-A5 early osteocytes. The reduction in TCF/LEF activity in co-cultures was more significant than that in osteoblast mono-cultures (Fig. 7). TCF/LEF activity in co-cultures was decreased by ~40% within 30 min of clinorotation, and it took < 1 h of clinorotation to achieve the same level of reduction at 4 h in the osteoblast mono-cultures. Also, the basal level of TCF/LEF activity at 0 h in co-cultures was substantially lower than that in mono-cultures (Fig. 7C). These results suggest that osteocytes are strong regulators of β-catenin signaling in clinorotated osteoblasts.

Discussion

The aim of the present study was to determine the effects of simulated unloading on β-catenin signaling and RhoA activity of osteoblasts. Using a FRET-based RhoA biosensor and a fluorescent TCF/LEF reporter, together with a custom-built clinorotation system that generates simulated weightlessness by averaging out a gravitational direction, we observed that the unloaded osteoblasts exhibited a decrease in RhoA activity and β-catenin signaling. These results are consistent with previous results using mesenchymal stem cells [26] as well as a study using hindlimb suspension models in mice, showing that Lef-1 and Cyclin D1, the targets of Wnt/β-catenin signaling, were decreased [43].

RhoA and TCF/LEF biosensors utilize different design strategies and expression mechanisms. Changes in RhoA activity (i.e., YFP/CFP emission ratio of the biosensor) are dependent on the conformational change of the biosensor, which can occur immediately following stimulation. On the other hand, changes in β-catenin signaling activity (i.e., expression of GFP) in the TCF/LEF biosensor is based on the transcription process involving several steps following stimulation: β-catenin stabilization and translocation, activation of TCF/LEF transcription factor, activation of Wnt-responsive gene and subsequent GFP expression in the cytoplasm. Therefore, we did not directly compare the temporal effects of clinorotation of RhoA and β-catenin signaling in this study. In order to directly compare the temporal activities of different signaling proteins, it might be desirable to use the biosensors that use a similar design strategy.

Our results using Wnt/β-catenin signaling inhibitor and RhoA mutants indicate that the endogenous basal level of β-catenin signaling is required for the down-regulation of RhoA, and that the basal levels of RhoA affects the temporal profile of activity and responsiveness of β-catenin signaling under simulated unloading. The inhibition of Wnt/β-catenin signaling using XAV939 significantly reduces the basal level of RhoA activity, resulting in the non-responsiveness of RhoA under simulated unloading. Previous reports show that RhoA is activated by Wnt3a, one of the canonical Wnt family members [44,45], and inhibition of intracellular β-catenin decreases RhoA activity [46]. On the other hand, osteoblasts transfected with constitutively active RhoA mutant increase the basal level of β-catenin signaling. Our data further suggests that the enhanced suppression of β-catenin signaling under simulated unloading observed in the osteoblasts transfected with constitutively active RhoA is due to the higher basal level of TCF/LEF activity in the cells. Consistently, recent reports demonstrated that activation of β-catenin is mediated by RhoA [47] and β-catenin-dependent induction of target genes is modulated by activated RhoA [45], suggesting the involvement of RhoA in β-catenin-dependent transcriptional pathway.

RhoA is known to regulate actin stress fibers and intracellular tension in many cell types including osteoblasts [48]. We have previously shown that RhoA is activated by fluid flow and its activation mediates fluid flow-induced PI3K and MAPK signaling [19]. In addition to actin, other cytoskeletal structures such as microtubules are also documented to play important roles in mechanotransduction [49]. Interestingly, we show here that, although RhoA mediates osteoblast response of β-catenin signaling to simulated unloading, actin structure and intracellular tension are not required in the β-catenin signaling activity. Currently, we do not know the mechanism, but other members of GTPases such as Rac1 [50,51] or other cytoskeletal structures [52,53] may be involved in Wnt/β-catenin signaling pathway.

We also observed that β-catenin signaling was significantly decreased in the osteocytes-osteoblasts co-cultures under clinorotation. Wnt/β-catenin signaling in osteoblasts is known to be regulated by sclerostin [42]. It is the protein product of Sost, exclusively expressed in osteocytes, and inhibits Wnt/β-catenin signaling pathway [54,55]. Recent reports using mice demonstrated a significant increase in Sost expression in hindlimb unloading experiments [12,43]. Together, these results suggest that Sost may serve as a mechanosensor and sclerostin release from osteocytes is an important factor to downregulate osteoblast response in Wnt/β-catenin signaling to unloading. In addition to this indirect, soluble factor-based communications from osteocytes to osteoblasts, cell-to-cell physical contact via connexin 43 [56,57] or N-cadherin [58,59] plays a crucial role in regulating osteoblastic activity such as alkaline phosphatase activity and β-catenin signaling.

In summary, the work presented here shows the experimental evidence that RhoA and β-catenin signaling interact under simulated unloading. Further studies are needed to investigate the effect of clinorotation on the expression of specific Wnt ligands (e.g., Wnt3a) or receptors and the role of other GTPases, such as Rac1 and Cdc42 in β-catenin signaling under clinorotation. In addition to elucidating the mechanism within osteoblasts, studies on interactions between osteocytes and osteoblasts through direct cell-cell contacts via gap

junctions or indirect contacts through a release of sclerostin from osteocytes will advance our understanding of β-catenin signaling under unloading.

Acknowledgments

We thank Dr. M. Matsuda (Kyoto University, Japan) and Dr. J. Miyazaki (Osaka University, Japan) for the gift of RhoA biosensor; Dr. R. Tsien (University of California, San Diego, CA) for the mCherry-actin; Dr. Y. Wang (University of Illinois, Urbana-Champaign, IL) for the RhoA mutants (RhoA-V14 and RhoA-N19). This work was supported by Indiana University-Purdue University Office of the Vice Chancellor for Research (S.N.), and National Institutes of Health Grant AR052144 (H.Y.).

References

1. Collet P, Uebelhart D, Vico L, Moro L, Hartmann D, et al. Effects of 1- and 6-month spaceflight on bone mass and biochemistry in two humans. Bone. 1997; 20:547–551. [PubMed: 9177869]
2. West JB. Physiology in microgravity. Journal of Applied Physiology. 2000; 89:379–384. [PubMed: 10904075]
3. Lang T, LeBlanc A, Evans H, Lu Y, Genant H, et al. Cortical and trabecular bone mineral loss from the spine and hip in long-duration spaceflight. Journal of Bone and Mineral Research. 2004; 19:1006–1012. [PubMed: 15125798]
4. LeBlanc A, Schneider V, Shackelford L, West S, Oganov V, et al. Bone mineral and lean tissue loss after long duration space flight. J Musculoskelet Neuronal Interact. 2000; 1:157–160. [PubMed: 15758512]
5. Minear S, Leucht P, Jiang J, Liu B, Zeng A, et al. Wnt proteins promote bone regeneration. Sci Transl Med. 2010; 2:29ra30.
6. Kim JB, Leucht P, Lam K, Luppen C, Ten Berge D, et al. Bone regeneration is regulated by wnt signaling. J Bone Miner Res. 2007; 22:1913–1923. [PubMed: 17696762]
7. Case N, Ma M, Sen B, Xie Z, Gross TS, et al. Beta-catenin levels influence rapid mechanical responses in osteoblasts. Journal of Biological Chemistry. 2008; 283:29196–29205. [PubMed: 18723514]
8. Norvell SM, Alvarez M, Bidwell JP, Pavalko FM. Fluid shear stress induces beta-catenin signaling in osteoblasts. Calcified Tissue International. 2004; 75:396–404. [PubMed: 15592796]
9. Behrens J, von Kries JP, Kuhl M, Bruhn L, Wedlich D, et al. Functional interaction of beta-catenin with the transcription factor LEF-1. Nature. 1996; 382:638–642. [PubMed: 8757136]
10. Bienz M, Clevers H. Armadillo/beta-catenin signals in the nucleus--proof beyond a reasonable doubt? Nat Cell Biol. 2003; 5:179–182. [PubMed: 12646868]
11. Mosimann C, Hausmann G, Basler K. Beta-catenin hits chromatin: regulation of Wnt target gene activation. Nat Rev Mol Cell Biol. 2009; 10:276–286. [PubMed: 19305417]
12. Robling AG, Niziolek PJ, Baldridge LA, Condon KW, Allen MR, et al. Mechanical stimulation of bone in vivo reduces osteocyte expression of Sost/sclerostin. J Biol Chem. 2008; 283:5866–5875. [PubMed: 18089564]
13. Robinson JA, Chatterjee-Kishore M, Yaworsky PJ, Cullen DM, Zhao W, et al. Wnt/beta-catenin signaling is a normal physiological response to mechanical loading in bone. J Biol Chem. 2006; 281:31720–31728. [PubMed: 16908522]
14. Jaffe AB, Hall A. Rho GTPases: biochemistry and biology. Annu Rev Cell Dev Biol. 2005; 21:247–269. [PubMed: 16212495]
15. Burridge K, Wennerberg K. Rho and Rac take center stage. Cell. 2004; 116:167–179. [PubMed: 14744429]
16. Yoshida T, Clark MF, Stern PH. The small GTPase RhoA is crucial for MC3T3-E1 osteoblastic cell survival. J Cell Biochem. 2009; 106:896–902. [PubMed: 19184980]
17. Chellaiah MA, Soga N, Swanson S, McAllister S, Alvarez U, et al. Rho-A is critical for osteoclast podosome organization, motility, and bone resorption. J Biol Chem. 2000; 275:11993–12002. [PubMed: 10766830]

18. Ohnaka K, Shimoda S, Nawata H, Shimokawa H, Kaibuchi K, et al. Pitavastatin enhanced BMP-2 and osteocalcin expression by inhibition of Rho-associated kinase in human osteoblasts. Biochem Biophys Res Commun. 2001; 287:337–342. [PubMed: 11554731]
19. Hamamura K, Swarnkar G, Tanjung N, Cho E, Li J, et al. RhoA-mediated signaling in mechanotransduction of osteoblasts. Connect Tissue Res. 2012; 53:398–406. [PubMed: 22420753]
20. Matthews BD, Overby DR, Mannix R, Ingber DE. Cellular adaptation to mechanical stress: role of integrins Rho, cytoskeletal tension and mechanosensitive ion channels. Journal of Cell Science. 2006; 119:508–518. [PubMed: 16443749]
21. Arnsdorf EJ, Tummala P, Kwon RY, Jacobs CR. Mechanically induced osteogenic differentiation--the role of RhoA, ROCKII and cytoskeletal dynamics. J Cell Sci. 2009; 122:546–553. [PubMed: 19174467]
22. Sambandam Y, Blanchard JJ, Daughtridge G, Kolb RJ, Shanmugarajan S, et al. Microarray profile of gene expression during osteoclast differentiation in modelled microgravity. Journal of Cellular Biochemistry. 2010; 111:1179–1187. [PubMed: 20717918]
23. Hashemi BB, Penkala JE, Vens C, Huls H, Cubbage M, et al. T cell activation responses are differentially regulated during clinorotation and in spaceflight. FASEB Journal. 1999; 13:2071–2082. [PubMed: 10544190]
24. Bucaro MA, Zahm AM, Risbud MV, Ayyaswamy PS, Mukundakrishnan K, et al. The effect of simulated microgravity on osteoblasts is independent of the induction of apoptosis. Journal of Cellular Biochemistry. 2007; 102:483–495. [PubMed: 17520667]
25. Pardo SJ, Patel MJ, Sykes MC, Platt MO, Boyd NL, et al. Simulated microgravity using the Random Positioning Machine inhibits differentiation and alters gene expression profiles of 2T3 preosteoblasts. Am J Physiol Cell Physiol. 2005; 288:C1211–C1221. [PubMed: 15689415]
26. Meyers VE, Zayzafoon M, Douglas JT, McDonald JM. RhoA and cytoskeletal disruption mediate reduced osteoblastogenesis and enhanced adipogenesis of human mesenchymal stem cells in modeled microgravity. J Bone Miner Res. 2005; 20:1858–1866. [PubMed: 16160744]
27. Yoshizaki H, Ohba Y, Kurokawa K, Itoh RE, Nakamura T, et al. Activity of Rho-family GTPases during cell division as visualized with FRET-based probes. J Cell Biol. 2003; 162:223–232. [PubMed: 12860967]
28. Na S, Chowdhury F, Tay B, Ouyang M, Gregor M, et al. Plectin contributes to mechanical properties of living cells. Am J Physiol Cell Physiol. 2009; 296:C868–C877. [PubMed: 19244477]
29. Hirata E, Yukinaga H, Kamioka Y, Arakawa Y, Miyamoto S, et al. In vivo fluorescence resonance energy transfer imaging reveals differential activation of Rho-family GTPases in glioblastoma cell invasion. Journal of Cell Science. 2012; 125:858–868. [PubMed: 22399802]
30. Li S, Chen BP, Azuma N, Hu YL, Wu SZ, et al. Distinct roles for the small GTPases Cdc42 and Rho in endothelial responses to shear stress. J Clin Invest. 1999; 103:1141–1150. [PubMed: 10207166]
31. Shaner NC, Campbell RE, Steinbach PA, Giepmans BN, Palmer AE, et al. Improved monomeric red, orange and yellow fluorescent proteins derived from Discosoma sp. red fluorescent protein. Nat Biotechnol. 2004; 22:1567–1572. [PubMed: 15558047]
32. Rosser J, Bonewald LF. Studying osteocyte function using the cell lines MLO-Y4 and MLO-A5. Methods Mol Biol. 2012; 816:67–81. [PubMed: 22130923]
33. Sambandam Y, Blanchard JJ, Daughtridge G, Kolb RJ, Shanmugarajan S, et al. Microarray profile of gene expression during osteoclast differentiation in modelled microgravity. J Cell Biochem. 2010; 111:1179–1187. [PubMed: 20717918]
34. Rambaut PC, Goode AW. Skeletal changes during space flight. Lancet. 1985; 2:1050–1052. [PubMed: 2865525]
35. Clevers H, van de Wetering M. TCF/LEF factor earn their wings. Trends Genet. 1997; 13:485–489. [PubMed: 9433138]
36. Buravkova LB, Romanov YA. The role of cytoskeleton in cell changes under condition of simulated microgravity. Acta Astronaut. 2001; 48:647–650. [PubMed: 11858272]
37. Carmeliet G, Bouillon R. The effect of microgravity on morphology and gene expression of osteoblasts in vitro. FASEB Journal. 1999; 13(Suppl):S129–S134. [PubMed: 10352154]

38. Hughes-Fulford M, Lewis ML. Effects of microgravity on osteoblast growth activation. Experimental Cell Research. 1996; 224:103–109. [PubMed: 8612673]
39. Huang SM, Mishina YM, Liu S, Cheung A, Stegmeier F, et al. Tankyrase inhibition stabilizes axin and antagonizes Wnt signalling. Nature. 2009; 461:614–620. [PubMed: 19759537]
40. Schlessinger K, Hall A, Tolwinski N. Wnt signaling pathways meet Rho GTPases. Genes Dev. 2009; 23:265–277. [PubMed: 19204114]
41. Santos A, Bakker AD, Zandieh-Doulabi B, Semeins CM, Klein-Nulend J. Pulsating fluid flow modulates gene expression of proteins involved in Wnt signaling pathways in osteocytes. J Orthop Res. 2009; 27:1280–1287. [PubMed: 19353691]
42. Li X, Zhang Y, Kang H, Liu W, Liu P, et al. Sclerostin binds to LRP5/6 and antagonizes canonical Wnt signaling. J Biol Chem. 2005; 280:19883–19887. [PubMed: 15778503]
43. Lin C, Jiang X, Dai Z, Guo X, Weng T, et al. Sclerostin mediates bone response to mechanical unloading through antagonizing Wnt/beta-catenin signaling. J Bone Miner Res. 2009; 24:1651–1661. [PubMed: 19419300]
44. Endo Y, Wolf V, Muraiso K, Kamijo K, Soon L, et al. Wnt-3a-dependent cell motility involves RhoA activation and is specifically regulated by dishevelled-2. J Biol Chem. 2005; 280:777–786. [PubMed: 15509575]
45. Rossol-Allison J, Stemmle LN, Swenson-Fields KI, Kelly P, Fields PE, et al. Rho GTPase activity modulates Wnt3a/beta-catenin signaling. Cell Signal. 2009; 21:1559–1568. [PubMed: 19482078]
46. Peng L, Li Y, Shusterman K, Kuehl M, Gibson CW. Wnt-RhoA signaling is involved in dental enamel development. Eur J Oral Sci. 2011; 119(Suppl 1):41–49. [PubMed: 22243225]
47. Langemeijer EV, Slinger E, de Munnik S, Schreiber A, Maussang D, et al. Constitutive ss-Catenin Signaling by the Viral Chemokine Receptor US28. PLoS One. 2012; 7:e48935. [PubMed: 23145028]
48. Kazmers NH, Ma SA, Yoshida T, Stern PH. Rho GTPase signaling and PTH 3–34, but not PTH 1–34, maintain the actin cytoskeleton and antagonize bisphosphonate effects in mouse osteoblastic MC3T3-E1 cells. Bone. 2009; 45:52–60. [PubMed: 19361585]
49. Na S, Collin O, Chowdhury F, Tay B, Ouyang M, et al. Rapid signal transduction in living cells is a unique feature of mechanotransduction. Proc Natl Acad Sci U S A. 2008; 105:6626–6631. [PubMed: 18456839]
50. Zhu G, Wang Y, Huang B, Liang J, Ding Y, et al. A Rac1/PAK1 cascade controls beta-catenin activation in colon cancer cells. Oncogene. 2012; 31:1001–1012. [PubMed: 21822311]
51. Wu X, Tu X, Joeng KS, Hilton MJ, Williams DA, et al. Rac1 activation controls nuclear localization of beta-catenin during canonical Wnt signaling. Cell. 2008; 133:340–353. [PubMed: 18423204]
52. Chen HJ, Lin CM, Lin CS, Perez-Olle R, Leung CL, et al. The role of microtubule actin cross-linking factor 1 (MACF1) in the Wnt signaling pathway. Genes Dev. 2006; 20:1933–1945. [PubMed: 16815997]
53. Rowning BA, Wells J, Wu M, Gerhart JC, Moon RT, et al. Microtubule-mediated transport of organelles and localization of beta-catenin to the future dorsal side of Xenopus eggs. Proc Natl Acad Sci U S A. 1997; 94:1224–1229. [PubMed: 9037034]
54. Winkler DG, Sutherland MK, Geoghegan JC, Yu C, Hayes T, et al. Osteocyte control of bone formation via sclerostin, a novel BMP antagonist. EMBO J. 2003; 22:6267–6276. [PubMed: 14633986]
55. van Bezooijen RL, Roelen BA, Visser A, van der Wee-Pals L, de Wilt E, et al. Sclerostin is an osteocyte-expressed negative regulator of bone formation, but not a classical BMP antagonist. J Exp Med. 2004; 199:805–814. [PubMed: 15024046]
56. Taylor AF, Saunders MM, Shingle DL, Cimbala JM, Zhou Z, et al. Mechanically stimulated osteocytes regulate osteoblastic activity via gap junctions. Am J Physiol Cell Physiol. 2007; 292:C545–C552. [PubMed: 16885390]
57. Grimston SK, Brodt MD, Silva MJ, Civitelli R. Attenuated response to in vivo mechanical loading in mice with conditional osteoblast ablation of the connexin43 gene (Gja1). J Bone Miner Res. 2008; 23:879–886. [PubMed: 18282131]

58. Castro CH, Shin CS, Stains JP, Cheng SL, Sheikh S, et al. Targeted expression of a dominant-negative N-cadherin in vivo delays peak bone mass and increases adipogenesis. J Cell Sci. 2004; 117:2853–2864. [PubMed: 15169841]

59. Ferrari SL, Traianedes K, Thorne M, Lafage-Proust MH, Genever P, et al. A role for N-cadherin in the development of the differentiated osteoblastic phenotype. J Bone Miner Res. 2000; 15:198–208. [PubMed: 10703921]

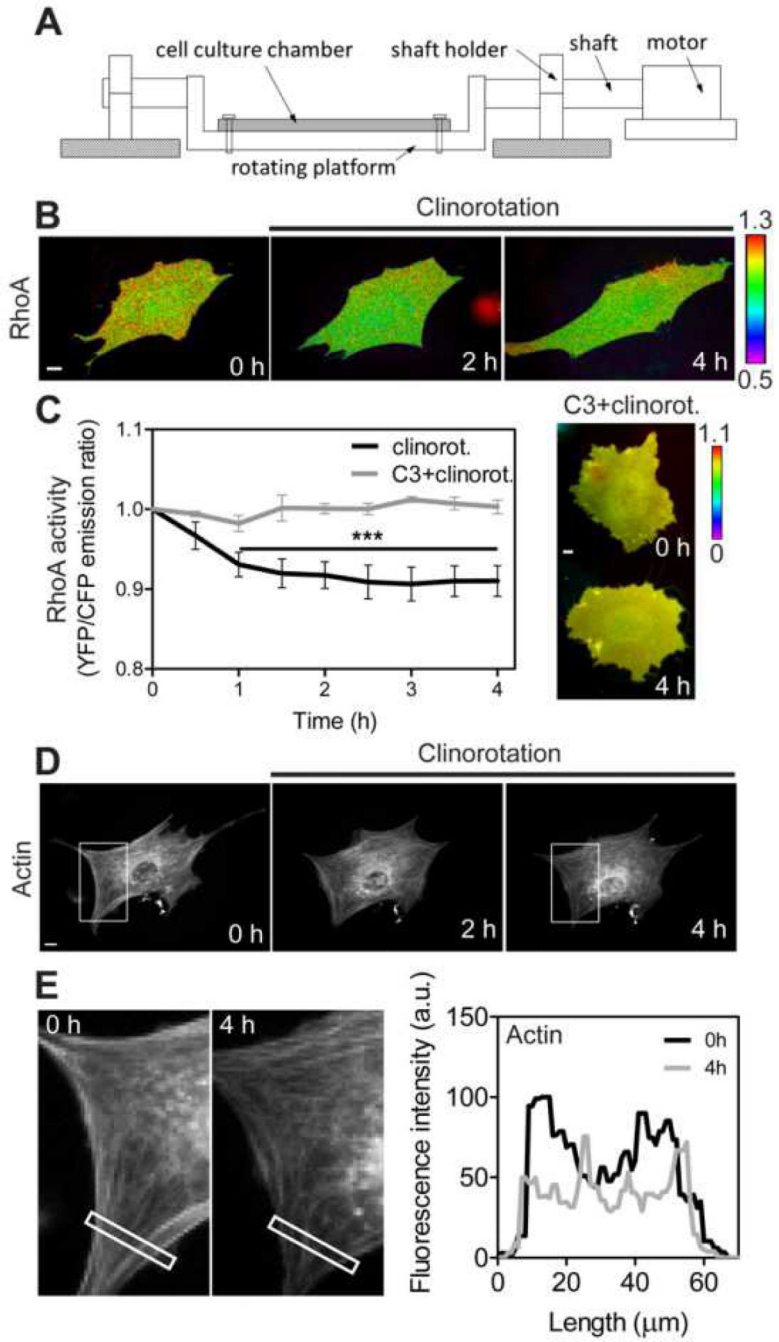

Fig. 1.

RhoA activity and actin cytoskeletal organization is downregulated under clinorotation. (A) A schematic of the custom-built clinostat. A cell culture chamber is mounted on the rotating platform. Clinorotation (simulated microgravity; 0.005 g) was achieved by using the platform with 2 cm of rotational radius (distance between the shaft and platform) and rotating the chamber at 15 rpm. (B) The FRET change of the RhoA biosensor in the representative MC3T3-E1 cell under clinorotation. The cell was transfected with a CFP-YFP RhoA biosensor. For each time-lapse imaging experiment the images from the same cell

were taken. Color bar represents emission ratio of YFP/CFP of the biosensor, an index of RhoA activation. Ratio images were scaled according to the corresponding color bar. (C) The time course represents RhoA activity of MC3T3-E1 cells under clinorotation. YFP/CFP emission ratios were averaged over the whole cell and were normalized to time 0. For the statistical analysis, emission ratios were compared with those at time 0 (*** $P < 0.001$). n = 10 cells. Rho inhibitor (C3)-treated cells did not show any changes in RhoA activity under clinorotation. n = 8 cells. (D) In response to clinorotation, MC3T3-E1 cell displays a decrease in actin structure. Five other cells showed similar results. The white boxes are cropped and enlarged for a better visualization in (E). (E) Fluorescence intensity profile of actin along the length of the rectangle from the left to the right at 0 h and 4 h of clinorotation. Scale bars = 10μm.

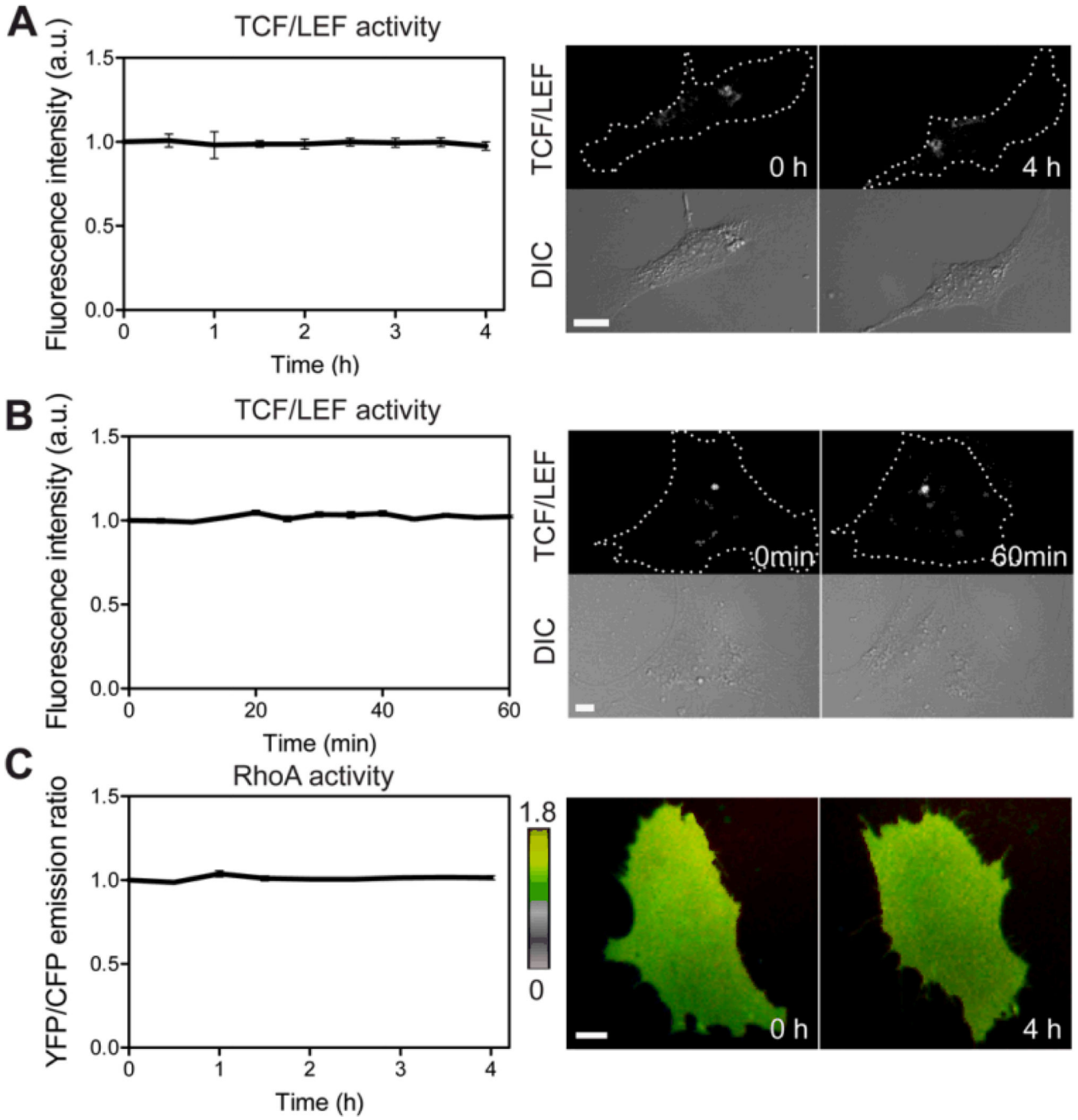

Fig. 2.

Static control experiments using MC3T3-E1 cells without applying clinorotation or shear stress. (A, B) TCF/LEF activities in the same experimental conditions used for clinorotation (A) or shear stress (B) experiments. (C) RhoA activity in the same experimental conditions used for clinorotation. *n* = 7 (A), 6 (B), 10 cells (C). Scale bars 10 μm.

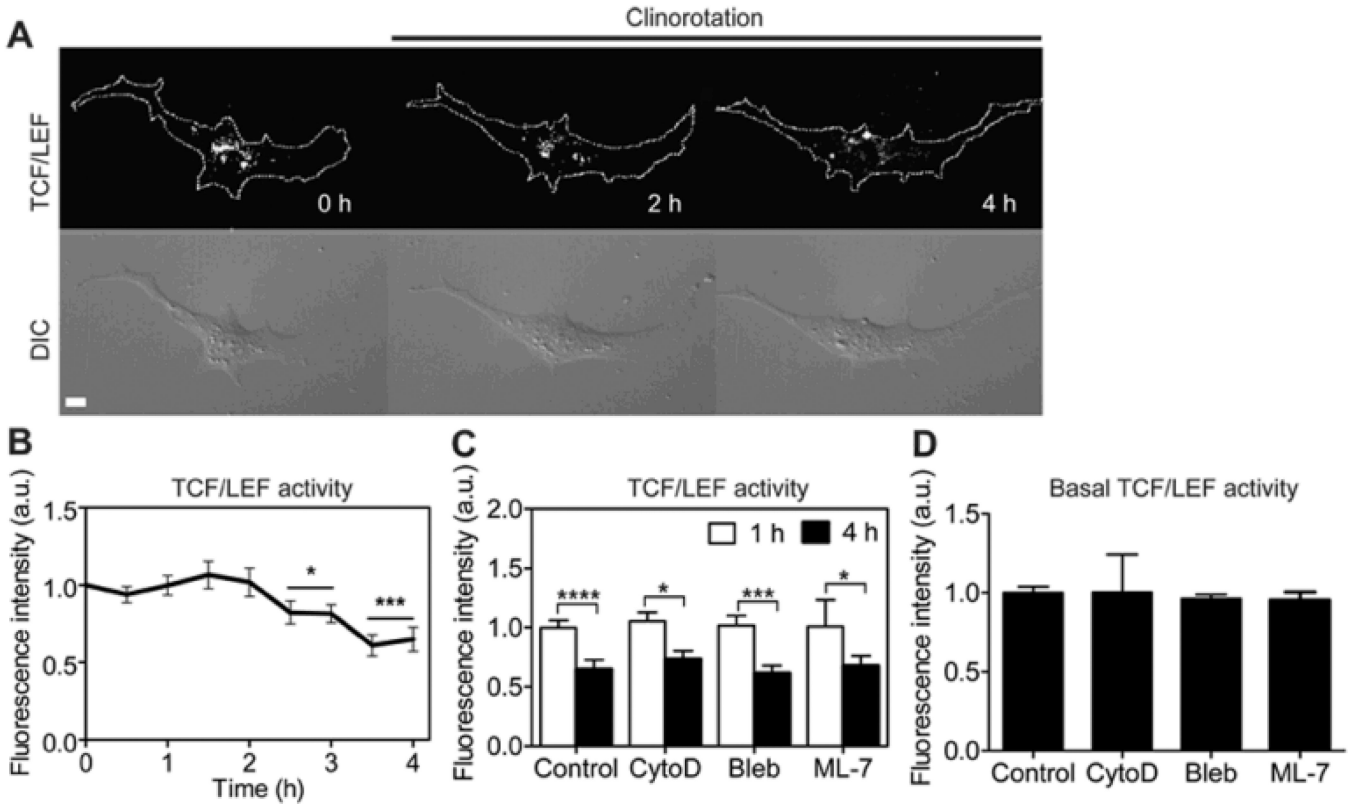

Fig. 3.

The effect of clinorotation on β-catenin signaling in MC3T3-E1 cells. (A) β-catenin signaling was determined by monitoring the fluorescence intensity of the cells transfected with the TCF/LEF-GFP reporter (See "Materials and methods"). For each time-lapse imaging experiment the images from the same cell were taken. Dashed lines in the top row images show cell boundaries which were obtained from the corresponding DIC images. Scale bar =10μm. (B) Fluorescence intensities of the TCF/LEF reporter were averaged over the whole cell and were normalized to time point 0 h. n = 10 cells. For the statistical analysis, TCF/LEF activities of the later time points were compared with that of 0 h (* P < 0.05, *** P < 0.001). (C) Bar graphs represent changes in TCF/LEF activity of the cells at 1 h and 4 h of clinorotation. The cells were transfected with a TCF/LEF reporter and then treated with CytoD (1μg/ml, n = 5 cells) to disrupt actin cytoskeleton, Bleb (50 μM, n = 5 cells) to inhibit myosin II, or ML-7 (25 μM, n = 5 cells) to inhibit MLCK. For the statistical analysis, TCF/LEF activities at 4 h were compared with the activity at 1 h for each condition (* P < 0.05, *** P < 0.001, **** P < 0.0001). (D) The basal level of TCF/LEF activity in the drug-treated cells. n = 10 (Control); 5 (CytoD); 5 (Bleb); 5 cells (ML-7).

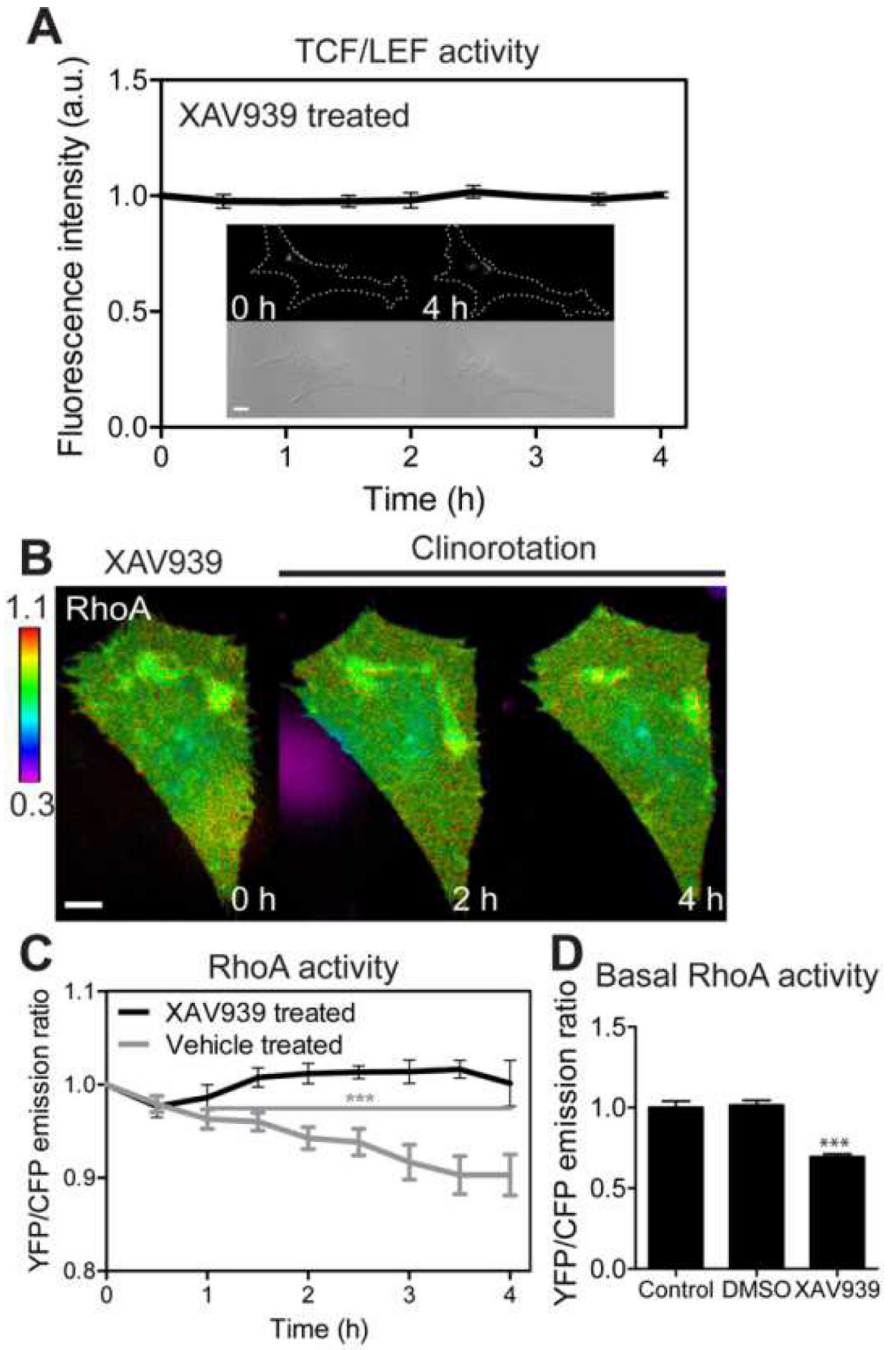

Fig. 4.

The role of β-catenin signaling on the RhoA activity by clinorotation. (A) TCF/LEF activity of XAV939-treated MC3T3-E1 cells under clinorotation. $n = 6$ cells. (B, C) RhoA activity of XAV939-treated MC3T3-E1 cells under clinorotation. RhoA activity failed to respond to simulated unloading. For statistical analysis of RhoA activity in vehicle (DMSO)-treated cells, the emission ratios were compared with those at time 0 (*** $P < 0.001$). $n = 6$ cells in both cases. (D) Basal RhoA activities of control cells, vehicle-treated cells, and XAV939-

treated cells. n = 10 (Control); 6 (DMSO); 7 cells (XAV939). *** $P < 0.001$. Scale bars 10μm.

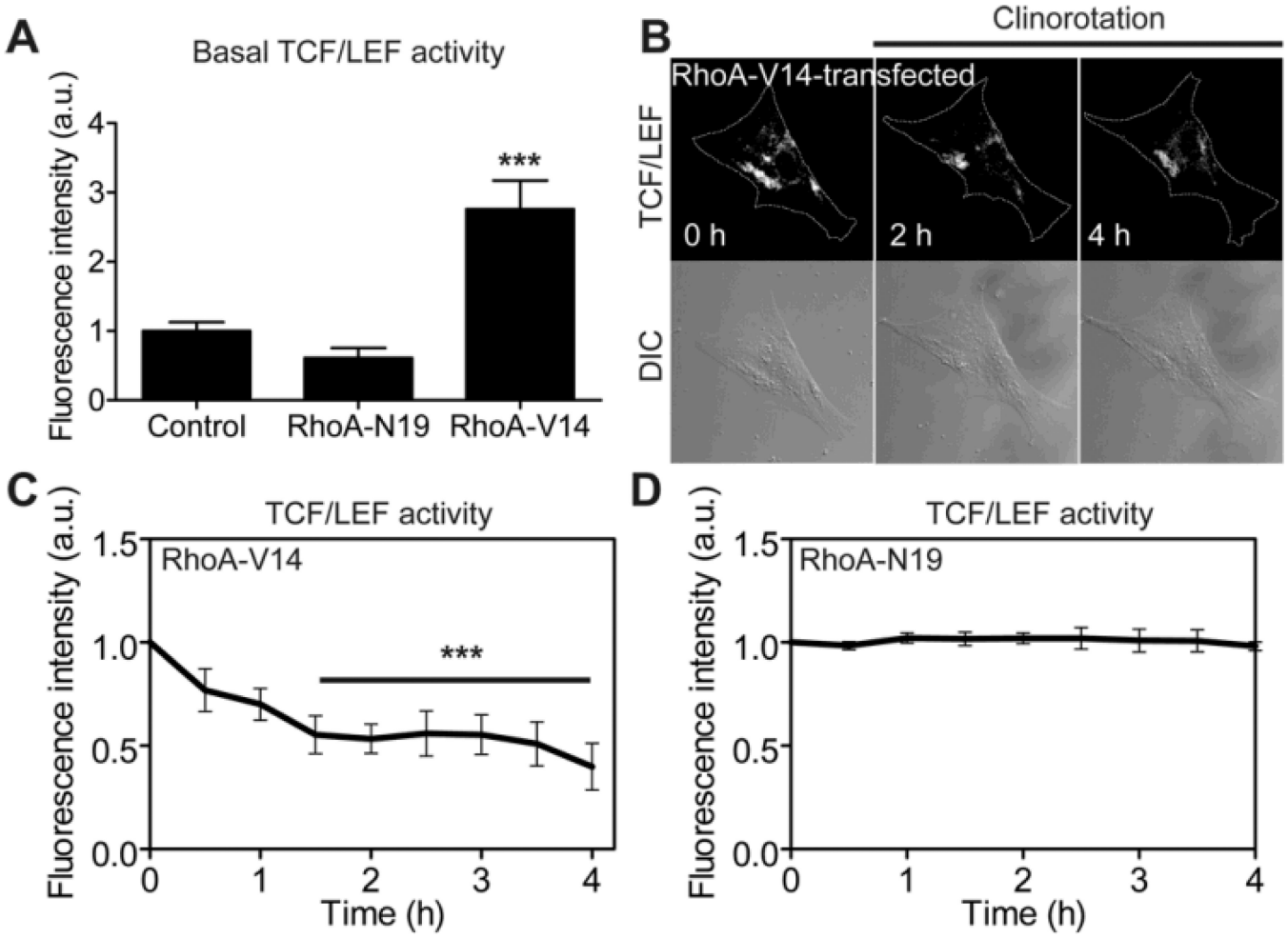

Fig. 5.

β-catenin signaling is rapidly, significantly reduced in MC3T3-E1 cells expressing constitutively active RhoA under clinorotation. (A) Basal TCF/LEF activities of control cells, and cells transfected with RhoA-N19 or RhoA-V14. RhoA-V14 data was compared with Control and RhoA-N19 data (*** $P < 0.001$). At least seven cells were analyzed. (B) β-catenin signaling was determined by monitoring the fluorescence intensity of the cells co-transfected with a TCF/LEF-GFP reporter and RhoA-V14. (C) Changes in TCF/LEF activity in response to clinorotation in MC3T3-E1 cells transfected with a constitutively active RhoA (RhoA-V14). $n = 7$ cells. For the statistical analysis, time course of TCF/LEF activity was compared with 0 hour (*** $P < 0.001$). (D) Changes in TCF/LEF activity in response to clinorotation in MC3T3-E1 cells transfected with a dominant negative RhoA (RhoA-N19). $n = 7$ cells.

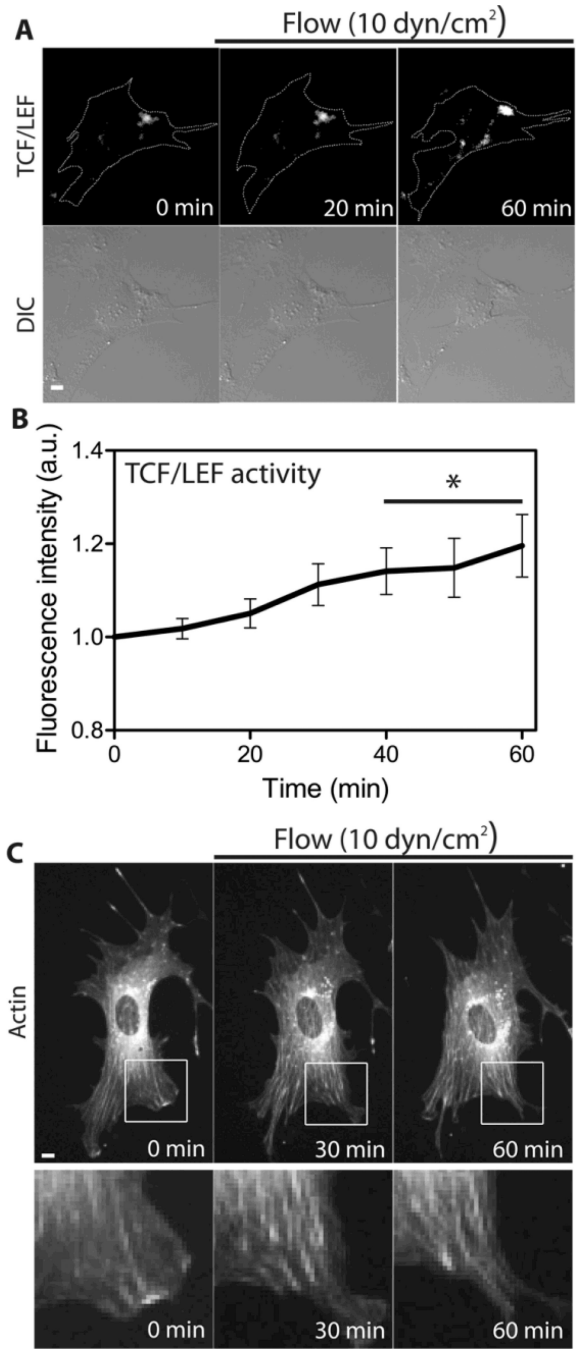

Fig. 6.

The effect of fluid flow on actin cytoskeletal organization and β-catenin signaling in MC3T3-E1 cells. (A, B) The time course of TCF/LEF activity in MC3T3-E1 cells in response to 10 dyn/cm^2 of shear stress. Scale bar =10μm. n = 5 cells. Time course of TCF/LEF activity was compared with 0 min (* $P < 0.05$). (C) In response to shear stress at 10 dyn/cm^2, the cell displays an increase in actin cytoskeleton structure. Six other cells showed similar results. The white boxes are cropped and enlarged for a better visualization. Scale bar 10μm.

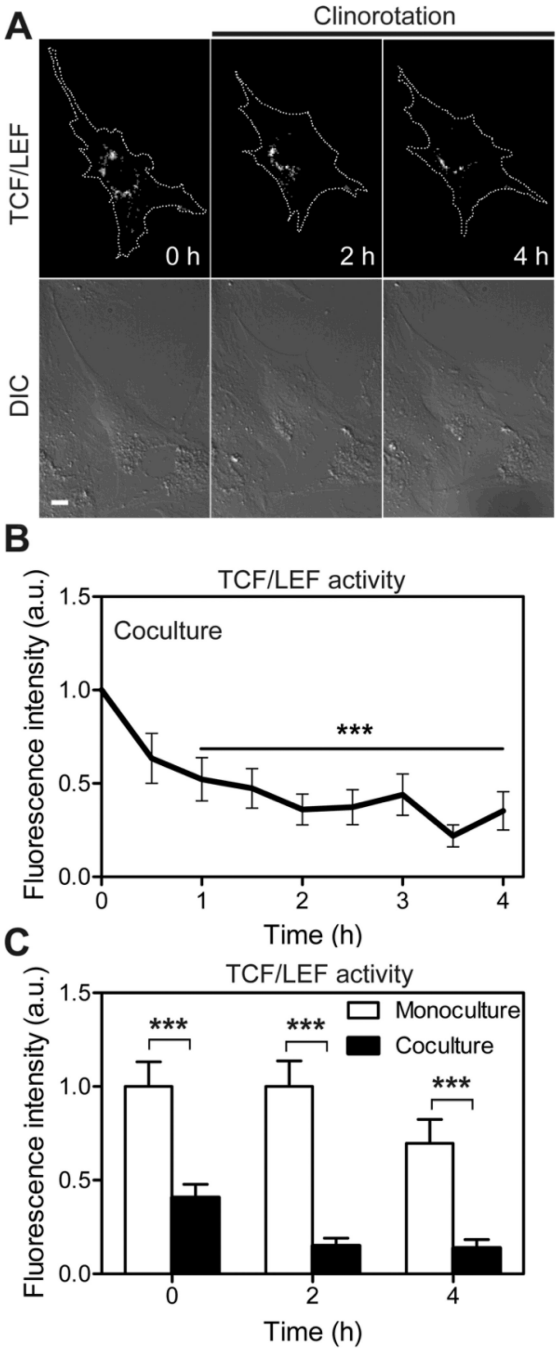

Fig. 7.

β-catenin signaling in MC3T3-E1 cells was dependent on the existence of osteocytes under clinorotation. (A) MC3T3-E1 cells cocultured with MLO-A5 cells were transfected with a TCF/LEF reporter and subjected to clinorotation for 4 h. Scale bar 10μm. (B) The time course of TCF/LEF activity in MC3T3-E1 cells in the cocultures under clinorotation. *** $P < 0.001$. $n = 7$ cells. (C) Bar graphs represent changes in TCF/LEF activity of MC3T3-E1 cells under clinorotation in the two different culture conditions (monocultures versus

cocultures) at three time points; 0, 2, and 4 h. Data were normalized to the basal TCF/LEF activity in monocultures at 0 h. *** $P < 0.001$. At least six cells were analyzed.